The Synergistic Mechanism of Antifreeze Proteins

Presented to the S. Daniel Abrahams Honors Program in Partial Fulfillment of the Requirements for the Completion of the Program

Stern College for Women

Yeshiva University

May 7, 2019

Tehilla Berger

Mentor: Dr. Ran Drori, Chemistry and Biochemistry

Table of Contents:

(i) Abstract

Antifreeze proteins and glycoproteins (AF(G)Ps) help cold-adapted organisms, such as fish, plants, and insects, to endure the subfreezing climates they preside in. These proteins bind to the surfaces of small ice crystals preventing further ice growth. Fish and insects use multiple AF(G)P isoforms, which vary greatly in their ability to inhibit ice. In some fish, the passive isoform that barely inhibits ice growth is more abundant than the active isoform. A synergistic enhancement of AF(G)Ps activity by mixture of two isoforms was revealed more than 40 years ago regarding AFGP (Osuga 1978) and AFPIIII (Takamichi 2009), but the mechanism that explains this phenomenon is still obscure. Using cold-stages, microfluidics, and fluorescence microscopy, we tested the activity of binary mixtures of AFPs from a fish and a plant. AFPIII and AFGP both exist in active and passive isoforms, and thus their passive isoforms were mixed with every active AF(G)P. Synergistic, additive, and antagonistic effects of the proteins' activity were observed for various binary mixtures. The passive protein AFPIII-SP showed synergy in all mixtures, with the exception of with AFPI, with which it showed additive activity. Passive $AFGP_{7\text{-}8}$ only showed synergy when mixed with the active AFGP, as well as with the passive form of AFPIII. However, when mixed with AFPI and *Lp*AFP, proteins with more moderate activity, antagonistic effects were observed. When the two active isoforms of AFGP and AFPIII were mixed, the results were antagonistic. Ice crystals that grew in microfluidic channels with a binary mixture of AFPIII isoforms tagged with different fluorescence dyes exhibited complementary binding to the prism and pyramidal planes of the crystal. Synergy was observed regardless of the AF(G)Ps' structure, suggesting that specific protein-protein interactions are not driving the activity enhancement or reduction. Synergistic enhancement was obtained in mixtures that included an active isoform, which binds rapidly to

the prism plane, and a slower passive isoform that binds to a pyramidal plane. The active isoform binds first to the prism plane, slows down growth and creates pyramidal surfaces, to which the passive isoform binds. This series of events leads to synergistically enhanced ice growth inhibition. In contrast, the AF(G)Ps that were antagonistic bind to the same ice-crystal plane, suggesting competition on the similar binding site. These results explain the mechanism of synergy between AF(G)P isoforms in binary mixtures, which is driven by complementary binding and a combination of rapid and slower adsorption rates to ice. These results are important to the AFP field as they identify a process that seems to exist in all AF(G)P-containing fish. While previous studies have highlighted the existence of synergy in isolated contexts, such as that of either AFPIII or AFGP (Osuga 1979, Zepeda 2008, Takamichi 2009), there has yet to be a conclusive and comprehensive statement regarding the mechanism of synergy in all fish. A cross-species synergy mechanism will be an exciting revelation in the field of AFPs and may explain other protein cooperative interactions. Discoveries in the field of antifreeze proteins not only further our understanding of how fish resist freezing of their bodily fluids, but have applications in preservation techniques, medicinal procedures, and technological advances. Antifreeze proteins have already been introduced as a proposed mechanism to preserve organs (Wang 1994) as well as for vitrification (Wowk 2000), and have been implemented in various food products (Boonsupthip 2003). AF(G)Ps thus influence a diverse range of specialties in a significant way.

(ii) Introduction

Antifreeze proteins and glycoproteins (AF(G)Ps) were first discovered when in 1969, it was determined that some Antarctic fish can survive temperatures as low as -1.87°C due to the presence of proteins containing carbohydrate groups (DeVries 1969). Since their initial exposé, the AF(G)P field has exploded with discoveries, as these proteins were identified in a myriad of organisms, such as fish (DeVries 1969), insects (Paterson 1979), plants (Arny 1977), bacteria (Gilbert 2004) , and fungi (Robinson 2001). Many organisms must be able to survive temperatures below 0°C, the freezing point of water, and AF(G)Ps function by adhering to the surface of small ice crystals, thereby inhibiting their growth by exhibiting thermal hysteresis (TH) activity, defined as the gap between ice's melting (T_m) and freezing (T_f) temperatures (Bar Dolev 2016). AF(G)Ps contain ice-shaping properties as well, as they bind to the surface of the ice crystals and alter their morphology (Figure 1). Despite the ubiquity of the ice-inhibiting function of AF(G)Ps, the structure and properties of actual proteins found in different organisms are eminently diverse (Davies 2014). This is a result of the various needs that AF(G)Ps serve in their host organisms. For instance, while fish only require TH activity of about 1°C (DeVries 1971), insects in cold climates can require TH activity of about 5°C, and therefore the AF(G)Ps found in insects exhibit far greater activity than those found in fish (Davies 2014).

A: Ice Shaping

In pure water, ice crystals grow in the shape of thin disks. Their circular, flat shape is due to ice's natural ability to expand equally in all directions along the *a*-axis, while growth along the *c*-axis is substantially slower. However, in the presence of even a miniscule amount

of AF(G)P, such that the concentration of protein would not be sufficient to inhibit ice growth, shaping is observed (Knight 2000). An Adsorption-Inhibition model explains this phenomenon by stating that as AF(G)Ps bind to the surface of the ice crystal, they create small curvatures, thus slowing ice growth (Raymond 1977). This effect will be explained in further detail in section ii(C). These AF(G)Ps bind preferentially to certain ice planes, and thus inhibit ice growth in the area in which the protein is bound. The hallmark of AF(G)Ps' binding is the shaping of ice-crystals, which varies among different proteins (Bar Dolev 2012).

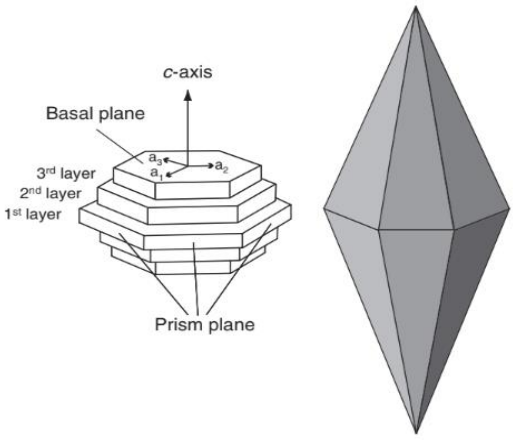

Figure 1. Bipyramidal crystal. Ice crystal growth morphology in the presence of fish AF(G)Ps.

The AF(G)Ps present in fish are moderate AF(G)Ps. Moderate AF(G)Ps can be distinguished from hyperactive AF(G)Ps, often found in insects, which exhibit TH activity up to 5°C, and have potent properties at low protein concentrations. In contrast, moderate AFP's have TH activity of about 1°C (DeVries 1971), and are only effective at much higher concentrations relative to hyperactive AF(G)Ps (Davies 2014). The characteristic shape of crystals in the presence of most moderate AF(G)Ps is a bipyramid (Bar Dolev 2016). Figure 1 shows that a crystal can grow in two directions: horizontally, referred to as an ice crystal's *a*-axis, or vertically, the *c*-axis. The plane that is perpendicular to the *a*-axis is referred to as the prism plane, while the basal plane is perpendicular to the *c*-axis. A third plane, the pyramidal plane, is the result of a developed bipyramidal shape, and may also be a site of protein binding. While hyperactive AF(G)Ps can bind to all ice surfaces and thereby exhibit lemon-like shapes,

moderate AF(G)Ps cannot bind to the basal plane (Drori 2015). As a result, ice growth can only occur along the *c*-axis. As ice growth continues at a constant rate in the c-direction, new prism surfaces will develop, and proteins will continue to bind to the new surfaces. Ice growth along the *c*-axis thus occurs in a step-like manner, with each step slightly smaller than the one preceding it, thereby inducing a bipyramidal shape. When the crystal's pyramidal planes merge and form a tip, which is composed of basal surfaces, ice growth is halted until it exhibits a significant burst along the *c*-axis. The temperature at which this burst occurs is referred to as the T_f point, the freezing point (Drori 2015).

B: Thermal Hysteresis Gap

The most important function of AF(G)Ps is their ability to form a gap between the melting point (T_m) and the T_f (Figure 2). This gap is a result of AF(G)Ps' binding to the surface of the ice crystal, which slows the growth of ice, causing it to shape and form tips before bursting. This gap is referred to as a thermal hysteresis gap (TH), and is a measure of AF(G)P activity (Bar Dolev 2016). While low concentrations of AF(G)P or passive AF(G)P isoforms have shaping properties, they are too weak to inhibit ice growth. However, in the absence of ice, there are no binding sites, and thus, the proteins have no activity (Bar Dolev 2016).

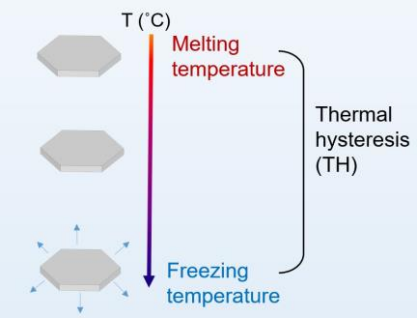

Figure 2: TH gap between melting and freezing temperatures. Below the melting point, ice crystals retain relative size, until the freezing temperature, when they experience a rapid burst.

C: Suggested Mechanism by which AFGP Binding Inhibits Ice Growth

The current suggested mechanism as to how AF(G)Ps bind to the surface of ice crystals is the Adsorption-Inhibition hypothesis (Raymond 1977). It utilizes the Gibbs-Thomson effect,

which is based on the second law of thermodynamics. The Gibbs-Thomson effect states that at the T_m or T_f of a crystal, water and ice are in a state of equilibrium, and thus, the Gibbs free energy of the system is zero. Because of this, we can deduce the following:

$$\Delta G_{ice} = 0 = H_{ice} - T\Delta S_{ice} = \Delta G_{water} = 0 = H_{water} - T\Delta S_{water}$$

$$T_m = \frac{\Delta H}{\Delta S} \qquad \text{(Equation 1)}$$

When proteins, or any solutes, are added to a solution of water and ice at equilibrium, they cause an increase in entropy (ΔS), and thus lower the T_m of the solution. This phenomenon is similar to the colligative effect, whereby adding solutes to a solution induces freezing point depression. However, AF(G)Ps are far more effective than the colligative property would allow, due to their other property, in which they induce curvatures in between binding sites of AF(G)Ps as a means of decreasing surface tension (Bar Dolev 2016). This, in turn, decreases the T_f, as is related by the following equation:

$$\Delta T = T_0 - T = \frac{2\Omega\Upsilon T_0}{p_{min}\Delta H_0} \qquad \text{(Equation 2)}$$

$T_0 - T$ represents the difference between the freezing temperature, T_f, and the melting temperature at equilibrium. ΔH_0 represents the heat of fusion, while Ω is the molar volume of ice. p_{min} is the radius of the curvature, and ϒ is the unit of surface tension, measured in (Force/unit length). This equation relates that as the radius of the surface of the ice crystal approaches infinity (the result of a flat surface), there will be no discrepancy between T_m and T_f. However, in the presence of a curvature at the surface, T_f will be depressed because its thermodynamically unfavorable for

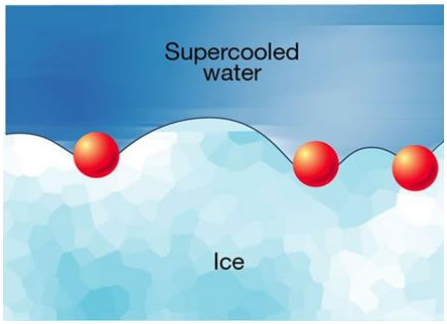

Figure 3: Curvatures Formed between adsorbed AFPs (Knight 2000).

water molecules to add to a curved surface, due to their decreased ability to form hydrogen bonds (Yeh 1996).

The Adsorption-Inhibition Model explains that AF(G)Ps bind to the growing surface of the ice, thus forcing water molecules to bind to the ice in between the locations of protein binding. This results in curved surfaces in between the binding sites of AF(G)Ps (Figure 3), which in turn, results in a lowering of the T_f of the ice crystals while T_m remains constant (Knight 2000).

D: How AFGPs Bind to Surface of Ice Crystal

The suggested mechanism of antifreeze protein adhesion to the surface of ice crystals is the Anchored-Clathrate Water Hypothesis (Nutt 2008). In this model, AF(G)Ps act as amphipathic molecules, and thus their hydrophilic group interacts with water in the solution. Their hydrophobic side then binds to the surface of the ice crystal while their hydrophilic side remains attached to a layer of ice-water from the solution (Nutt 2008).

There is much debate as to whether or not AF(G)Ps bind irreversibly to ice. One theory suggests that the binding of AFGPs to the ice-surface is due to hydrophobic interactions, and thus, their binding is reversible (Mochizuki 2018). Similarly, using NMR to observe the molecules on the ice-surface, AFPs were found to bind reversibly as well (Ba 2003). However, this theory is in dissonance with an experiment performed using microfluidics devices to examine ice inhibition of AFGPs while its surrounding protein containing solution was replaced by buffer. The results of this experiment showed that proteins remained bound to the ice surface, and thus suggests irreversible binding (Drori 2015). This same method was further used to test AFPs, which were found to be irreversible as well (Celik 2013).

E: Structures of AF(G)Ps

AF(G)Ps in different organisms exhibit unique structures. Figure 4 illustrates the characteristic structures of AF(G)Ps. AFPI (4a) are found in winter flounder and consist of a singular alpha-helix and are 3.3 kDa in length. Their primary sequence contains a high percentage of the amino acid alanine. AFPIII (4b) exist in multiple isoforms and are found in Arctic fish, but are most prevalent as AFPIII-SP, an inactive isoform, and AFPIII-QAE, an isoform with high activity. Their structures contain one alpha-helix, short beta strands, and one beta-clip fold. They have a total length of 7 kDa (Bar Dolev 2016). The active and inactive of AFPIII forms differ in amino acid sequence by 41 percent, with the active form rich in flexible amino acids such as valine and leucine, which are assumed to be involved in the ice-binding process (Takamichi 2009). *Lp*AFPs (4c), AFPs that are found in grass, consist of a secondary structure that is exclusively beta-solenoid, are composed of 118 amino acid residues, and contain a total of 8 turns (Bar Dolev 2016). AFGPs (4d) are native to Antarctic fish. While they have not yet been crystalized, AFGP monomers consist of three amino acid residues connected to an amino-methyl sugar residue. AFGPs also exist in an active and passive form. The active isoform, $AFGP_{1\text{-}5}$, contains 16-52 monomeric units, while the passive isoform, $AFGP_{7\text{-}8}$, has 4-5 units. In addition to the difference in the length of the

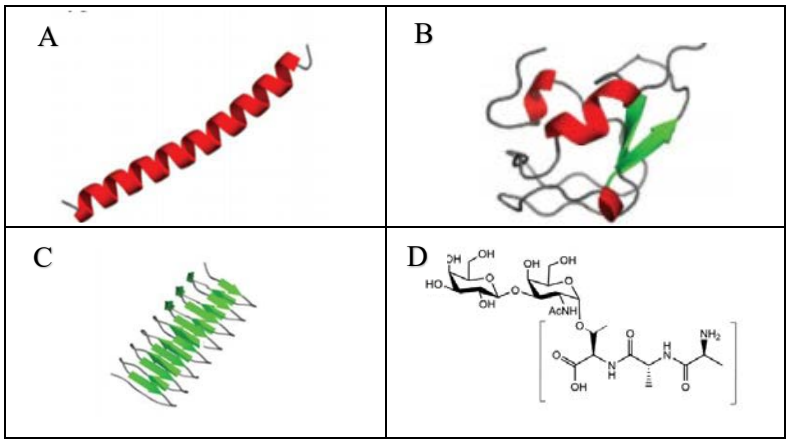

Figure 4: **Structures of Various Antifreeze Proteins**. A) the structure of AFPI (Bar Dolev 2016). B) the generalized structure of AFPIII (Bar Dolev 2016). C) the structure of *Lp*AFP (Bar Dolev 2016). D) represents a monomer of an AFGP.

peptide, the $AFGP_{7-8}$ differs from its active isoform in that it often contains proline and arginine, two amino acids that disrupt protein folding (Osuga 1978).

F: Crystal-Plane Binding Sites

In addition to differing in structure, AF(G)Ps do not all bind to the same ice-crystal planes (Bar Dolev 2016). Moderate AF(G)Ps can bind to the prism or pyramidal ice-crystal planes, or to both. Different isoforms of the same AF(G)P can also differ in crystal-plane binding. $AFGP_{1-5}$, AFPIII-QAE, and *Lp*AFP all bind to the prism planes of ice crystals. AFPI (Knight 1991) and AFPIII-SP can only bind to the pyramidal planes, while $AFGP_{7-8}$ has been reported to bind to both the prism and pyramidal plane (Knight 1993).

G: Applications of AF(G)Ps

AF(G)Ps have applications in many fields, such as medicine, biotechnology, agriculture, and the food industry. In medicine, AF(G)Ps have been shown to improve prolonged cryopreservation of organs, though experimentation has not yet passed animal models (Wang 1994). Additionally, they have been shown to be advantageous in egg and sperm vitrification (Wowk 2000). However, the extent of the adverse effects of AF(G)Ps in humans, such as toxicity and autoimmune responses, have not yet been determined. In biotechnology, AF(G)Ps are currently being explored for preventing the icing of roads (Esser-Kahn 2010). While this research is still in its elementary stages, AF(G)Ps can potentially provide a major safety advantage if they are incorporated into roads or other public surfaces that are dangerous when icy. In agriculture, they can provide freeze-resistant abilities to plants, and thus allow them to be grown in new locations with new climates (Bar Dolev 2016). In the food industry, AF(G)Ps have been successfully introduced into frozen foods, like ice cream,

to inhibit recrystallization of large ice crystals. This has allowed companies like Breyers® to create fat free ice cream with a very smooth consistency (Unilever). Because the field of AF(G)Ps remains relatively new, additional applications are likely to surface.

H: Alternate Ice-Growth Inhibiting Substances

Because of the many functions AF(G)Ps may serve, research has been conducted to find other substances that can serve similar ice inhibiting roles, while being more readily available and less costly. Polyvinyl alcohol, zirconium acetate, and zirconium acetate hydroxide have been found to have properties of ice shaping, and can prevent the recrystallization of ice crystals, much like AF(G)Ps (Bar Dolev 2016). The dye, Safranine, was shown to induce TH activity as well (Drori 2016).

I: Synergy Found in AF(G)Ps

An interesting phenomenon has been found in Arctic and Antarctic fish, whereby although each contain active and passive isoforms of AF(G)Ps, the majority of the AF(G)Ps in these fish are the passive isoform. In Arctic fish, the active protein isoform is AFPIII-QAE, while the passive isoform is AFPIII-SP. AFPIII-SP alone has no TH activity, although it does induce crystal shaping. Previous research has shown synergy between the active and passive isoforms, as the addition of 1% of AFPIII-QAE to a mixture of AFPIII-SP produces significant TH activity (Takamichi 2009).

Similarly, in Antarctic fish, $AFGP_{7\text{-}8}$, the passive isoform, is more abundant than $AFGP_{1\text{-}5}$, the active isoform. Unlike AFPIII-SP, $AFGP_{7\text{-}8}$ does produce TH activity, although it is minimal. In 1978, David Osuga showed there to be synergy between $AFGP_{1\text{-}5}$ and $AFGP_8$ ($AFGP_{7\text{-}8}$ is a mixture of $AFGP_7$ and $AFGP_8$, which produce very similar activity). Mixtures

of 1 mg/mL of $AFGP_{1-5}$ were added to concentrations of $AFGP_8$ ranging from 1 to 70 mg/mL, and synergy was observed at all concentrations (Osuga 1978).

J: Research Goals and Hypothesis

While the theory of synergy explains the abundance of the less active form of glycoproteins in fish, the mechanism by which it functions has yet to be determined. The mechanism of synergistic TH activity might work by one of two of the following hypotheses: firstly, the two isoforms interact and bind to each other before binding to ice (protein-protein interaction), or alternatively, the active form binds first to the ice surface before the passive isoform binds to the ice surface, and there is no interaction between the two isoforms (protein-ice interaction). To study the mechanism of synergy, passive and active isoforms of different types of AF(G)Ps were tested for synergy in a binary mixture. Because of the diverse nature of the structures of AF(G)Ps, if synergy is found between the active and passive isoforms of different AF(G)Ps, we can preclude the possibility of protein-protein interaction as the cause of synergy, as the drastically different structures are unlikely to interact with one another. If true, the mechanism of synergy will therefore be a result of the way in which the different isoforms bind to the surface of the ice, and may be a result of alternate-plane binding. This is the first time a correlation has been drawn between the synergy in fish with AFPs and those with AFGPs, and thus introduces a novel synergistic mechanism that occurs in all Arctic and Antarctic fish containing AF(G)Ps.

(iii) Materials and Methods

This research uses a combination of methods including microfluidics, cold-stages and fluorescently-labeled AF(G)P. TH measurements utilize a cold-stage, an upright microscope, and a temperature sensitive osmometer. Microfluidics allows us to isolate microns-sized ice crystals and control their temperature using a sensitive temperature control apparatus (Figure 5). The AFGPs and AFPI were obtained as part of a collaboration with Konrad Meister (AMOLF institute, the Netherlands) and Art DeVries (University of Illinois). The AFPIII isoforms and *Lp*AFP were obtained from Peter Davies (Queens' University).

A: TH Measurement Setup

In order to allow accurate temperature measurements up to ±0.002°C, a software was developed based on the design of Drori and Braslavsky (2013). This experimental design uses an upright microscope, coupled with a sensitive camera, and LabVIEW Software (Figure 5). The software allows the sample to quickly freeze when set to a temperature of -25°C, a current of 100A, and a voltage of 3.5 V. It must be set to -25°C due to the supercooling effect. When the whole sample freezes over, it can be melted rapidly to -8±2°C, at which point the current and voltage are changed to 10 A and 2.0 V, respectively. This allows for more controlled, incremental melting.

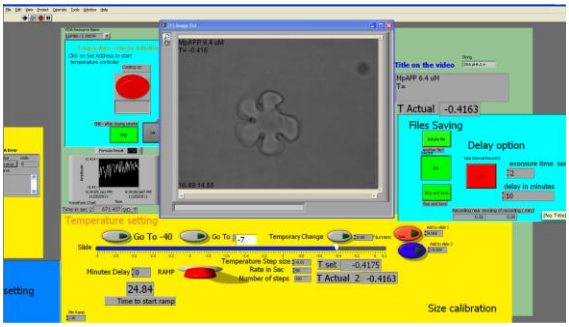

Figure 5. LabVIEW Software (Braslavsky 2013).

The upright microscope is connected to a Sony CMOS camera with a resolution of 2.3 MP. The cold-stage (Figure 6) is connected to a cooling apparatus, which allows cold water to

enter the plate through the water inlet and collects the warm water exiting the stage through the water outlet. The water cools the thermoelectric coolers, which in turn, cool the copper plate which contains the copper disk into which the sample is added. The copper disk contains a thermistor, which can be read by the LabVIEW program, and allows the temperature to be measured and adjusted accurately. Additionally, the cold-stage is attached to nitrogen gas, which prevents condensation on the sample.

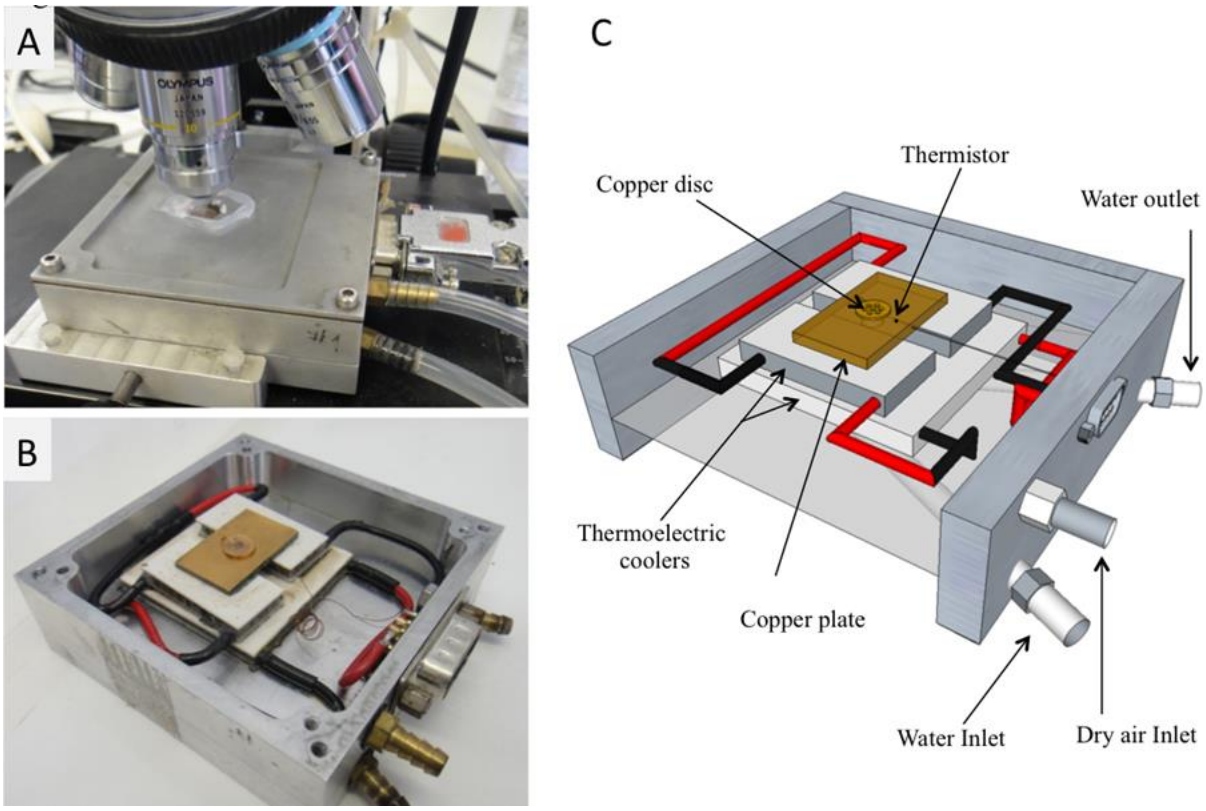

Figure 6: Microscope and Cold-Stage Setup. A represents the inverted microscope, B depicts an actual Cold-Stage setup, while C represents the a sketch of the design. (Image obtained from Braslavsky 2013).

The copper disc itself is 1 mm thick, and contains seven identical holes, each 500 µm in diameter. The disc is covered in immersion oil, and placed on the copper plate, such that each hole is filled with oil, and can be viewed by the camera. Protein samples can then be added to a hole using a capillary tube and syringe, resulting in sample sizes of 50-100 µm, and individual crystals of 10 µm. The sample is then frozen, and partially melted so that one

isolated ice-crystal remains. The melting temperature, the temperature just above which melting occurs, is recorded, and the temperature is lowered at a fixed rate (0.005 °C per 4 seconds). The ramp is allowed to run until the crystal begins to burst (T_f), and that temperature is recorded as well.

B: Microfluidics and Fluorescently Labeled Proteins

Microfluidics allows tiny fluid samples to be studied and manipulated using channels that are micrometers in size (Whiteside 2006). A special device design was devised to study AF(G)Ps (Figure 7). This allows samples to be examined in the tiny channels, in addition to allowing the exchange of solutions through the two inlets and the outlet.

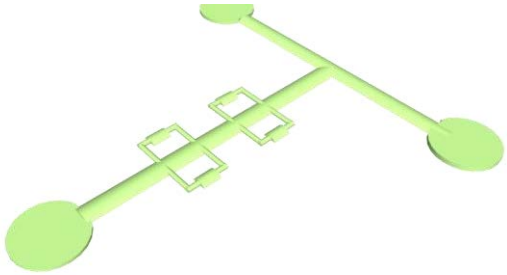

Figure 7: Unique Microfluidics Device designed for study of AF(G)Ps.

The device is prepared by pouring a mixture of polydimethylsiloxan (PDMS), (prepared according to package instructions) onto a prepared mold containing the desired design (Figure 7). PDMS is unique in that although it is a solid at room temperature, fluids may flow within it. The PDMS solution is allowed to dry in a dessicator, to prevent airbubbles from forming. After an hour, the device is removed, and three holes are punctured to create the inlets and outlet neccesary for fluid flow. The device is then placed on a cover slip and heated at a low temperature, until the device has completely adhered to the glass. The device is then cleaned with a buffer solution and tested for any leakage. 1% BSA solution is then injected into the apparatus for 20 minutes, to eliminate increased fluorescent signals on the walls of the device. It is then rinsed with buffer once again, and then is ready for use.

Microfluidics devices and TH measurments utilize a similar cold-stage apparatus (Figure 6). However, microfluidics requires an inverted fluorescent microscope, and instead of the sample being placed on a copper disk, it is placed on a transparent sapphire disk which is coated in immersion oil to increase thermal conductivity. The device is placed on the sapphire disk, and is taped down to ensure that it does not move while being tested. Each inlet and outlet is connected to a tube. One inlet is connected to protein, and the other to buffer. Using a syringe, the desired sample can be inserted into the device and studied, thus allowing for exchange of protein and buffer when desired. Once the sample is frozen, ice crystals can be isolated using a 980 nm IR laser.

Fluorescent labeling and microscopy allows the effects of different proteins in the mixture to be observed. The two fluorescent labels utilized were Tetramethyl Rhodamine (TRITC) and Fluorescein Isothiocyanate (FITC). TRIC is a dye that absorbs light in the orange spectrum when excited, and emits purple light, while FITC absorbs light in the blue spectrum, and emits light in the green spectrum. Because different proteins are labeled with different dyes in a mixture, different wavelengths of the dyes allow each protein to be imaged independently on the same crystal, allowing for observations of protein binding in mixtures.

D: Formation of Binary Mixtures and TH Analysis

Binary mixtures were formed between active $AFGP_{1\text{-}5}$, AFPIII-QAE, AFPI, and *Lp*AFP with two passive isoforms, $AFGP_{7\text{-}8}$ and AFPIII-SP. Concentrations of the active forms were chosen so that the TH of the pure form was $0.1 \pm .027$°C. A constant concentration of the active form was added to five increasing concentrations of the passive form, and five TH experiments were performed for each concentration. A mixture of $AFGP_{1\text{-}5}$ and AFPIII-QAE was formed as well, adding consistent amounts of AFPIII-QAE to $AFGP_{1\text{-}5}$. Each graph

included a logarithmic curve of the expected value of the results, which reflects the activity of an additive mixture.

C: Combination Index Calculation

In order to mathematically verify the presence of synergy or antagonism in a binary mixture, a formula (Equation 3) has been derived to give numerical significance to the apparent activity of mixtures at different concentrations (Farmanesh 2014).

$$Combination\ index = \frac{C_{1mixture}}{C_{1\ individual}} + \frac{C_{2\ measured}}{C_{2\ expected}} \quad \text{(Equation 3)}$$

The computed number is referred to as the Combination Index (CI). The first fraction in the equation is used to compute the CI for the active isoform. $C_{1\ mixture}$ is the concentration of the active isoform in a mixture that results in a certain activity, while $C_{1\ individual}$ is the concentration of the pure active isoform that would be required to obtain the same activity. The second fraction is used to compute the CI of the passive isoform. $C_{2\ measured}$ is the activity of a particular concentration in a mixture, while $C_{2\ expected}$ is the expected TH of the mixture used, which is calculated by adding the TH values of the concentrations of the pure isoforms in isolation.

The resulting combination index can be interpreted as follows: A mixture CI with a value below 1 can be classified as antagonistic, while one with a CI above 1 ±0.1 would be synergistic. When CI is equal to 1, the mixture displays additivity.

(iv) Results

The data represented below is original in its entirety. All TH measurements (Figures 8-16) were performed in Dr. Ran Drori's lab at Stern College for Women between February 2018 and March 2019 by Tehilla Berger. The microfluidics experiments (Figure 16) were performed

in conjunction with Dr. Ran Drori, while the calculations of the combination indexes (Figure 15) were performed entirely by Dr. Ran Drori.

A: Thermal Hysteresis Measurements

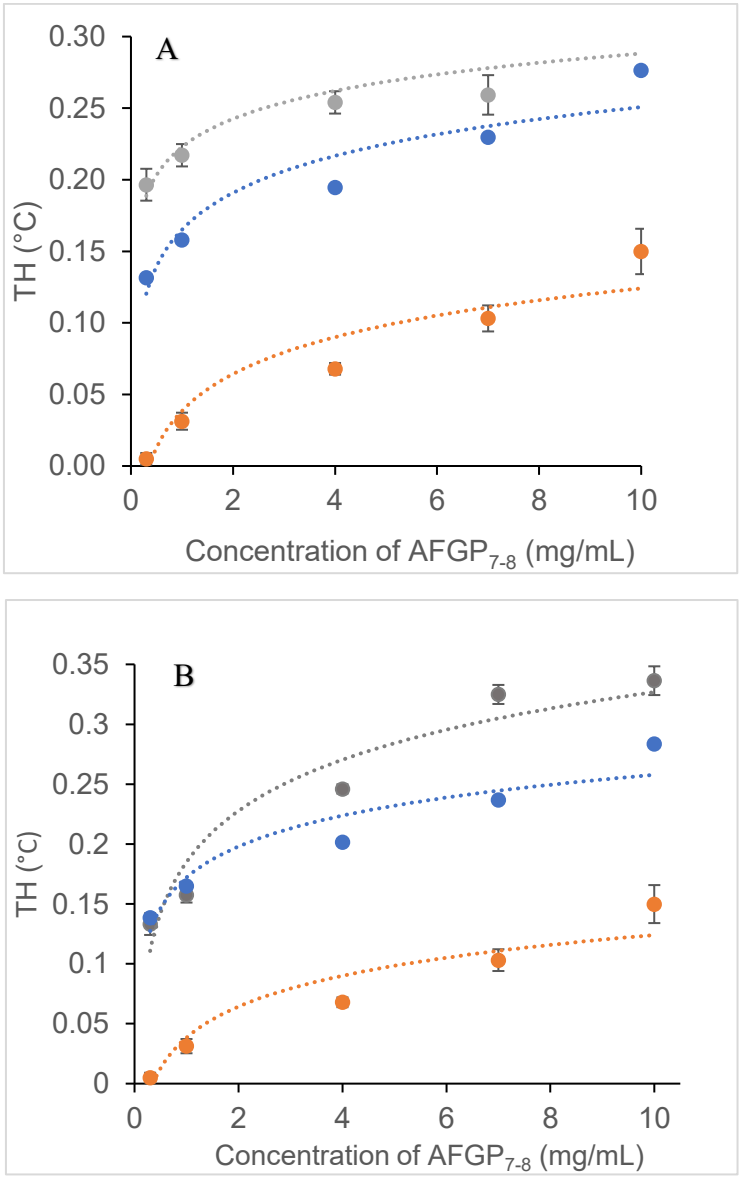

Figure 8: Synergy of AFGP$_{7\text{-}8}$. (A) Exhibits the binary mixture of AFGP$_{7\text{-}8}$ mixed with 1.0 mg/mL AFGP$_{1\text{-}5}$. The grey line represents the values obtained. The blue curve illustrates the expected values, while the orange represents the experimental values of pure AFGP$_{7\text{-}8}$. (B) exhibits the binary mixture of AFGP$_{7\text{-}8}$ mixed with 0.09 mg/mL AFPIII-QAE, depicted in grey. The blue line represents the expected values, while the orange represents pure AFGP$_{7\text{-}8}$.

<u>Highly Synergistic Protein Mixtures</u>

Figure 8(a) demonstrates the effect of mixing 1.0 mg/mL of AFGP$_{1\text{-}5}$, the active isoform, with increasing concentrations of AFGP$_{7\text{-}8}$, ranging from 0.3 to 10 mg/mL. The results exhibit synergy, evidenced by the experimental values creating a logarithmic curve above that of the expected value, though the efficacy of the synergy begins to decrease as concentrations of the passive isoform increase. Note that each data point represents five experiments, and the error bars represent the standard error. This finding is consistent with

previous research, which found cooperative binding between $AFGP_{1-5}$ and $AFGP_{8}$, though the $AFGP_{7-8}$ isoform was not tested (Osuga 1978). Figure 8(b) shows similar synergy between $AFGP_{7-8}$ and AFPIII-QAE. Mixtures were prepared with 0.09 mg/mL of AFPIII-QAE and increasing concentrations of $AFGP_{7-8}$, again ranging from 0.3 to 10 mg/mL. The expected TH was the additive of the activity of pure $AFGP_{7-8}$ at each concentration, as well as the activity of 0.09 mg/mL AFPIII-QAE, 0.09°C. This concentration of AFPIII-QAE was chosen for measurement in order to allow for comparison of the synergistic effects of AFPIII-QAE and $AFGP_{1-5}$ on $AFGP_{7-8}$, as its TH is very close to $AFGP_{1-5}$'s TH of 0.1266°C used above. The results exhibited synergy when the concentration of $AFGP_{7-8}$ was above 1 mg/mL, while below this concentration, the mixtures displayed additive activity. The synergistic effect appears to increase gradually as concentrations increase, and the extent of synergy exhibited seems greater than that of the $AFGP_{7-8}$ and $AFGP_{1-5}$ mixture.

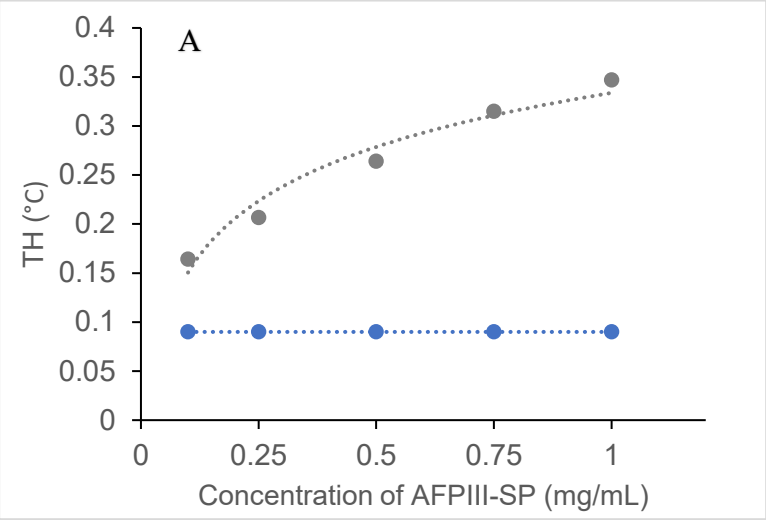

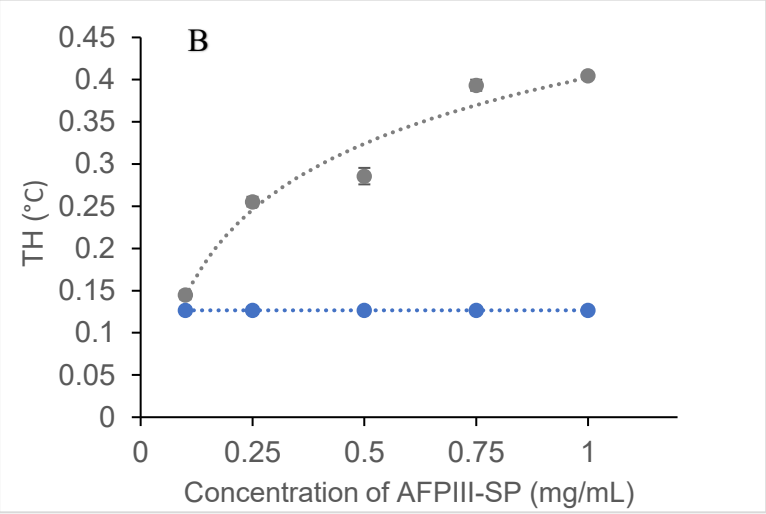

Figure 9: Synergy of AFPIII. (A) exhibits the synergy in a binary mixture of AFPIII-SP mixed with 0.09 mg/mL AFPIII-QAE. The grey line represents the values obtained. The blue curve illustrates the expected values. (B) exhibits values between a binary mixture of AFPIII-SP and 1.0 mg/mL $AFGP_{1-5}$. The grey curve represents the experimental values obtained while the blue line represents the expected value.

Similarly, Figure 9 shows synergy between AFPIII-SP when mixed with AFPIII-QAE (9a), as well as when mixed with $AFGP_{1-5}$ (9b). In Figure 9a, the error was so miniscule, that while the bars are present, they are not visible. AFPIII-SP and AFPIII-QAE mixture was formed by adding 0.09 mg/mL of AFPIII-QAE to increasing concentrations of AFPIII-SP, ranging from 0.1 to 1.0 mg/mL. The expected TH is equal to the TH of AFPIII-QAE at 0.09 mg/ml (0.09 °C), as AFPIII-SP does not exhibit any TH. However, when the active and passive isoforms are mixed, the inactive isoform begins to exhibit significant TH activity, and increases consistently within the range of concentrations tested. This finding is consistent with previous research that the inactive form becomes activated in the presence of very small amounts of AFPIII-QAE (Takamichi 2009). Similarly,

mixtures of AFPIII-SP and 1.0 mg/mL of $AFGP_{1-5}$ display synergy (9b). The expected activity was 0.1266°C, the activity of pure 1.0 mg/mL of $AFGP_{1-5}$ at all concentrations of SP. However, much like was observed in mixtures of AFPIII-SP and QAE (Figure 9a), AFPIII-SP exhibits increasing TH activity as its own concentration increases, while the $AFGP_{1-5}$ remains constant. This increase in activity indicates that when mixed with the active isoform of AFGP, the otherwise inactive AFPIII-SP obtains significant activity.

Moderately Synergistic Protein Mixtures

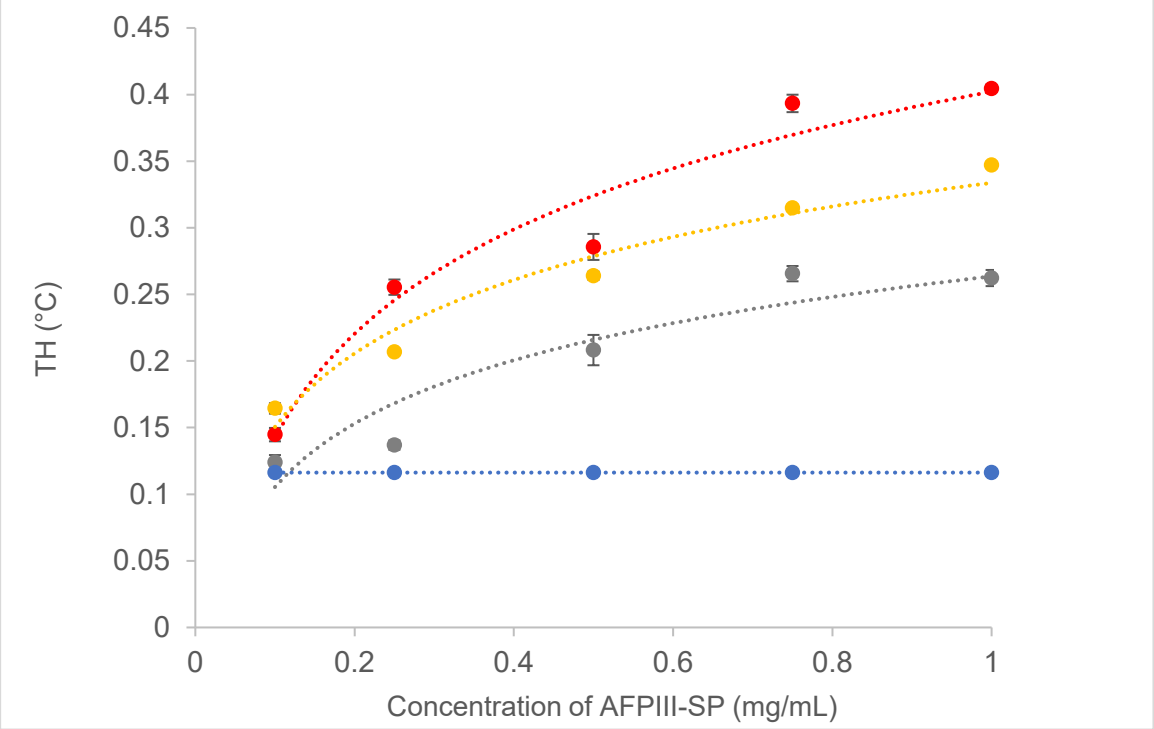

Figure 10. Mixture of *Lp*AFP with AFPIII-SP. The grey curve represents a binary mixture of AFPIII-SP and 0.5 mg/mL of *Lp*AFP. The blue line represents the expected values. The orange line represents a mixture of AFPIII-SP and 1 mg/mL $AFGP_{1-5}$, while the red represents a mixture of AFPIII-SP and 0.09 mg/mL of AFPIII-QAE.

Figure 10 shows that *Lp*AFP exhibits some limited amount of synergy when mixed with AFPIII-SP. Mixtures of *Lp*AFP and AFPIII-SP were prepared by adding 0.5 mg/mL of *Lp*AFP to increasing concentrations of AFPIII-SP, ranging from 0.1 to 1 mg/mL. The

concentration of *Lp*AFP was chosen as its TH is 0.1162°C. Because AFPIII-SP alone shows no TH activity, the expected TH value was that of pure 0.1 mg/mL *Lp*AFP. While the synergy exhibited is enough to be considered significant and increases as concentration increases, the synergy exhibited is significantly less than that exhibited when AFPIII-SP was mixed with AFPIII-QAE and $AFGP_{1\text{-}5}$. This is evident in Figure 10, where the yellow and red lines represent mixtures of AFPIII-SP with $AFGP_{1\text{-}5}$ and AFPIII-QAE, respectively, both of which exhibit greater synergistic enhancement than the binary mixture of AFPIII-SP and *Lp*AFP, represented in grey. Therefore, the mixture of AFPIII-SP and *Lp*AFP is best characterized as moderately synergistic, as although it exhibits synergistic activity, it has less synergistic enhancement than mixtures of AFPIII-SP with $AFGP_{1\text{-}5}$ or AFPIII-QAE.

Mixture with Additive Effect

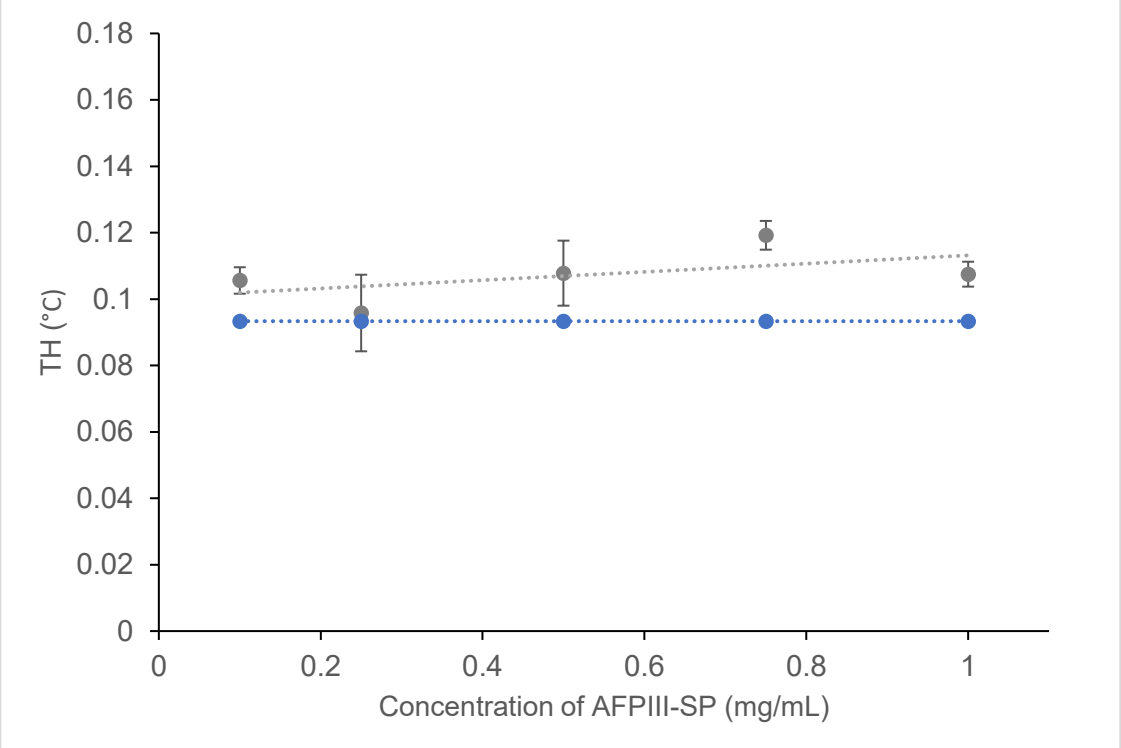

Figure 11: Mixture of AFPI with AFPIII-SP. The grey line depicts the TH activity of a binary mixture of AFPIII-SP and 0.2 mg/mL of AFPI. The blue line represents the expected TH, that of pure 0.2 mg/mL AFPI.

Figure 11 shows that although AFPI is relatively active in comparison to AFPIII-SP, upon mixing, no synergy is observed. Mixtures of inactive AFPIII-SP and AFPI were prepared with a constant concentration of 0.2 mg/mL of AFPI and increasing concentrations of AFPIII-SP from 0.1 to 1 mg/mL. Because the pure form of AFPIII-SP is inactive, the expected TH was that of pure 0.2 mg/mL AFPI, which was experimentally determined to be 0.093°C, and therefore, the plot is linear. The results plotted in Figure 10 show no synergy, as the measured activity is very similar to the expected activity. It therefore appears as though AFPIII-SP remains inactive when mixed with AFPI. These results are in consonance with those obtained in Figure 12 below, where a mixture of a passive isoform with AFPI does not induce synergy.

Antagonistic Mixtures

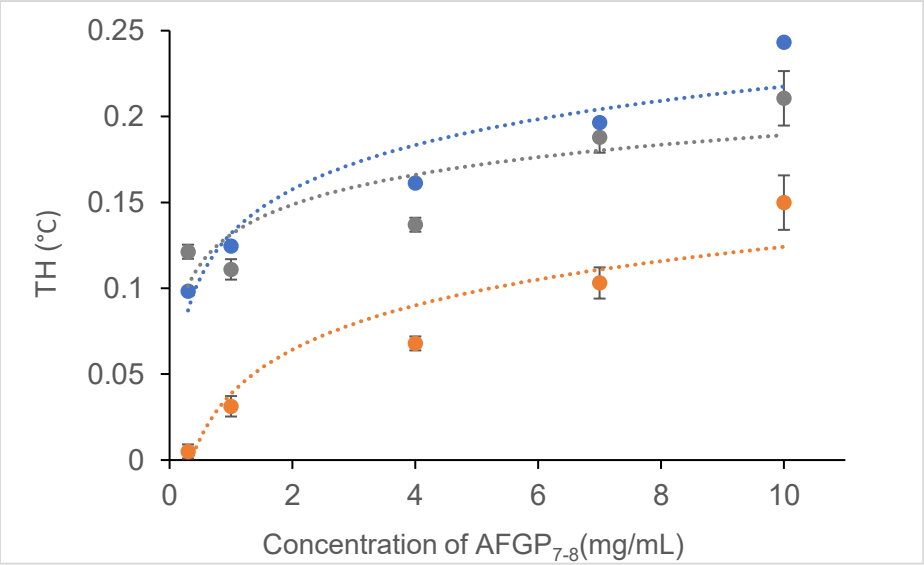

Figure 12. Mixture of $AFGP_{7\text{-}8}$ and AFPI. The grey curve illustrates the TH activity of a binary mixture of $AFGP_{7\text{-}8}$ and 0.2 mg/mL AFPI. The blue curve represents the expected values, while the orange depicts the TH activity of pure $AFGP_{7\text{-}8}$.

Figure 12 illustrates that in a mixture, $AFGP_{7-8}$ and AFPI are antagonistic to one another, despite AFPI being far more active then $AFGP_{7-8}$. A mixture of 0.2 mg/mL of AFPI and $AFGP_{7-8}$ with concentrations ranging from 0.3 to 10 mg/mL was tested. The measured activity was similar to the expected activity, namely, the additive activity of both proteins in the mixture. The TH activity of 0.2 mg/mL of AFPI is 0.093 °C, and thus this value was added to the values of pure $AFGP_{7-8}$ at every measured concentration to obtain the expected TH curve. As the concentrations of $AFGP_{7-8}$ increase, the experimental values begin to deviate from the expected ones, as evidenced in the growing gap between the gray and blue curves in the Figure (12). It appears that at higher concentrations, AFPI and $AFGP_{7-8}$ act in an antagonistic fashion, but based on TH measurements alone, within the range of concentrations tested, it is hard to determine definitively if that is the case, as the standard error for these experiments was relatively large.

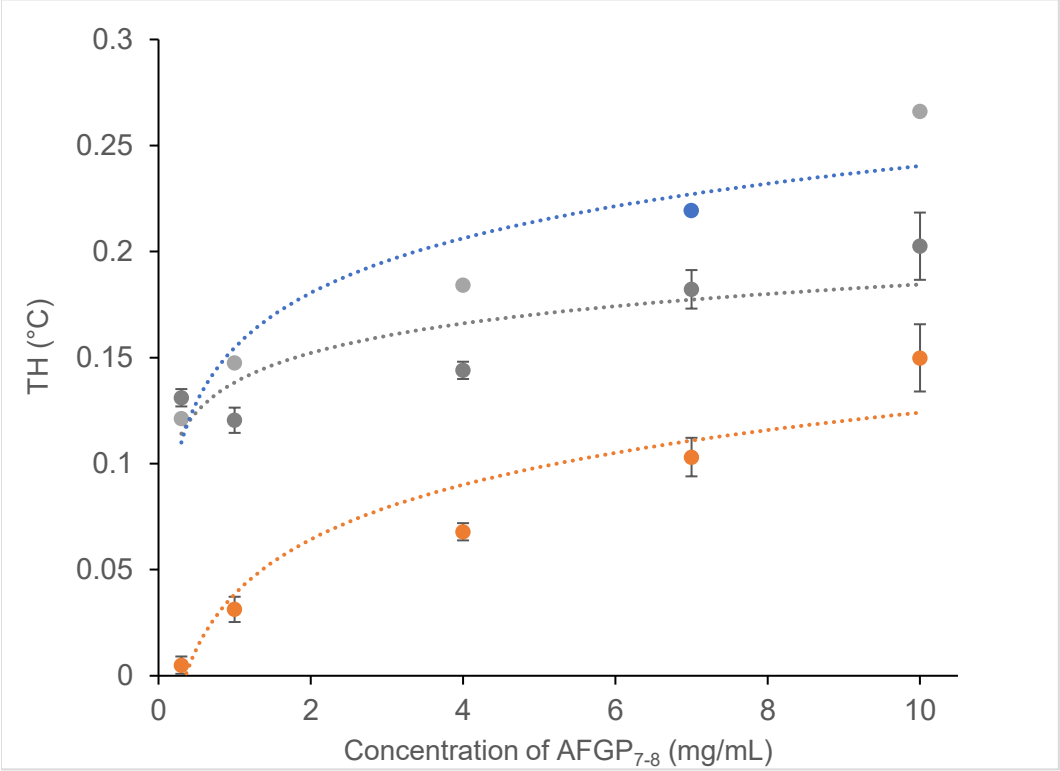

Figure 13: $AFGP_{7-8}$ with *Lp*AFP. The grey curve represents the TH activity of a binary mixture of AFGP 7-8 and 0.5 mg/mL of *Lp*AFP. The blue curve represents the expected values, while the orange represents the TH activity of pure $AFGP_{7-8}$.

Figure 13 highlights the antagonism between $AFGP_{7\text{-}8}$ and *Lp*AFP in a mixture. Although *Lp*AFP is far more active then $AFGP_{7\text{-}8}$, the addition of 0.5 mg/mL *Lp*AFP (TH of 0.1162°C) to incrementally increasing concentrations of $AFGP_{7\text{-}8}$, ranging from 0.3 to 10 mg/mL resulting in a lower activity then expected. The expected activity is calculated based on the addition of the activities of the pure forms. Since the activity is lower than expected, the proteins can be said to be antagonistic to one another. It appears as though as the concentration of $AFGP_{7\text{-}8}$ increases, the mixture becomes increasingly antagonistic.

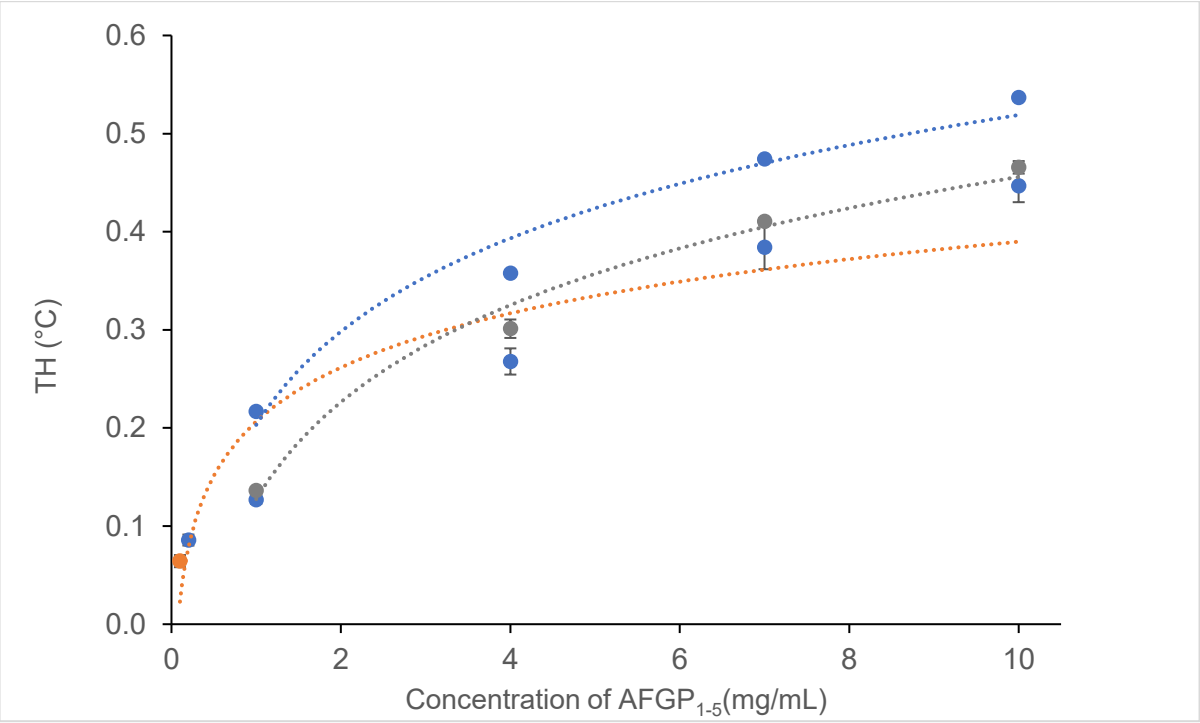

Figure 14: Mixture of $AFGP_{1\text{-}5}$ and AFPIII-QAE. The grey curve represents the TH activity of binary mixture $AFGP_{1\text{-}5}$ and 0.09 mg/mL of AFPIII-QAE. The blue curve represents the expected TH, while the orange represents the activity of pure $AFGP_{1\text{-}5}$.

Figure 14 exemplifies that when two active proteins are mixed, the resulting activity is lower than the additive activity of a mixture of $AFGP_{1\text{-}5}$ and AFPIII-QAE with a steady

concentration of 0.09 mg/mL of QAE (TH of 0.09°C) and concentrations of $AFGP_{1-5}$ ranging from 0.1 mg/mL to 10 mg/mL. Again, each data point is representative of five TH measurements, with the error bars depicting the standard error of those experiments. The concentration of AFPIII-QAE was chosen as its TH value is close to 0.1°C. The expected TH was the additive activity of the pure protein forms. The mixture remained consistently antagonistic as the concentration of $AFGP_{1-5}$ increased.

B: Calculation of the Combination Index

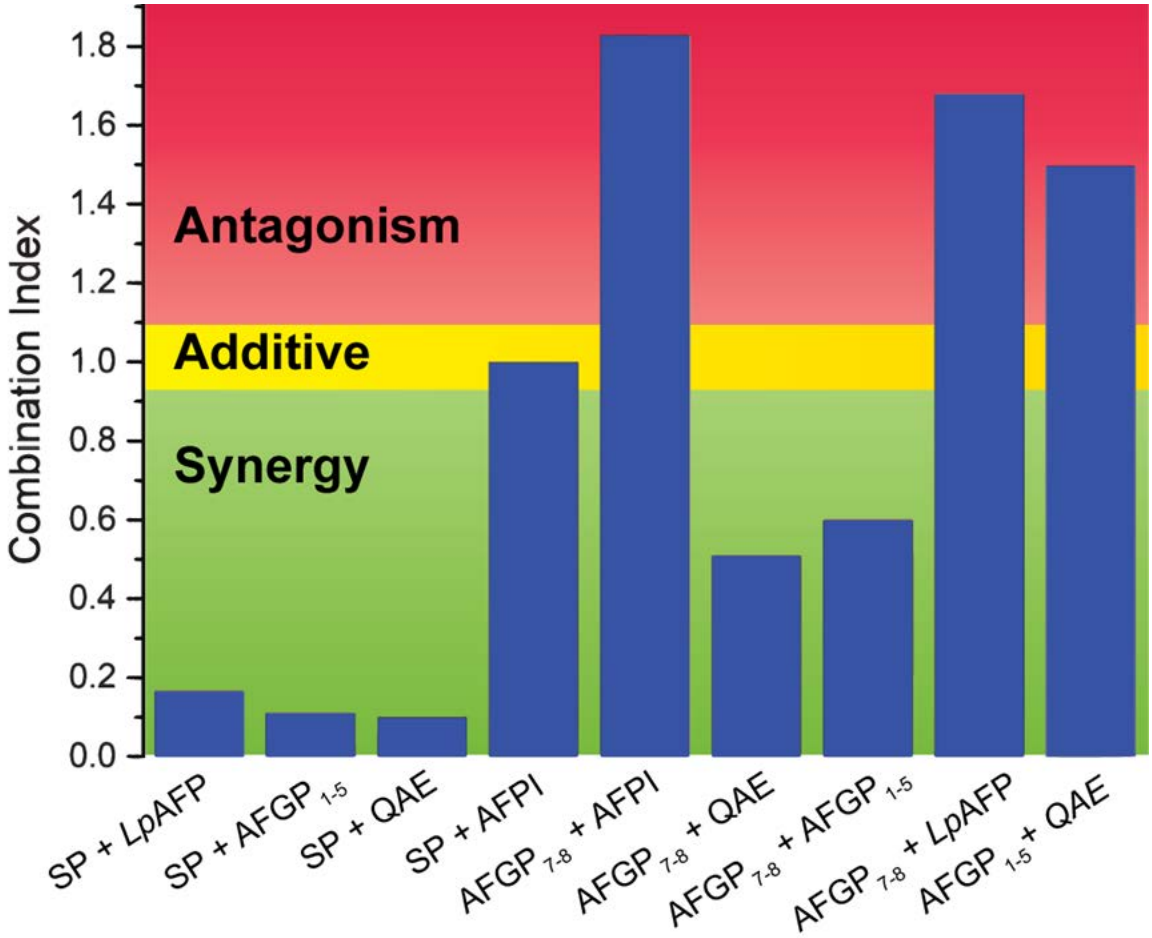

Figure 15: Combination Indexes of all protein mixtures. Combination Indexes were calculated using Equation 3. Synergy is determined by values below 1, additive by 1±0.1, and antagonist by values above one. On the x-axis, the passive protein tested at increasing concentrations of the binary mixture is listed first.

The bar graph in Figure 15 mathematically confirms the different mixtures' additive, antagonistic, and synergistic properties based on Equation 3. These calculations allow the synergistic properties of different binary mixtures to be precisely compared to one another. More negative Combination Indexes indicate stronger synergy, and thus it appears as though AFPIII-SP and AFPIII-QAE form the most synergistic mixture. Mixtures of $AFGP_{1-5}$ and AFPIII produce an almost identical level of synergy, while that of *Lp*AFP and AFPIII-SP is significant, but appreciably lower. Mixtures of $AFGP_{7-8}$ and AFPIII-QAE exhibit more synergy than $AFGP_{7-8}$ mixed with $AFGP_{1-5}$. Interestingly, while mixtures of AFPI and AFPIII-SP show an additive effect in mixture, $AFGP_{7-8}$ and AFPI produce the most antagonistic combination tested. Additionally, $AFGP_{7-8}$ is antagonistic, albeit to a lesser extent, when mixed with *Lp*AFP. When two active isoforms, $AFGP_{1-5}$ and AFPIII-QAE, are mixed, they are strongly antagonistic as well.

C: Microfluidics

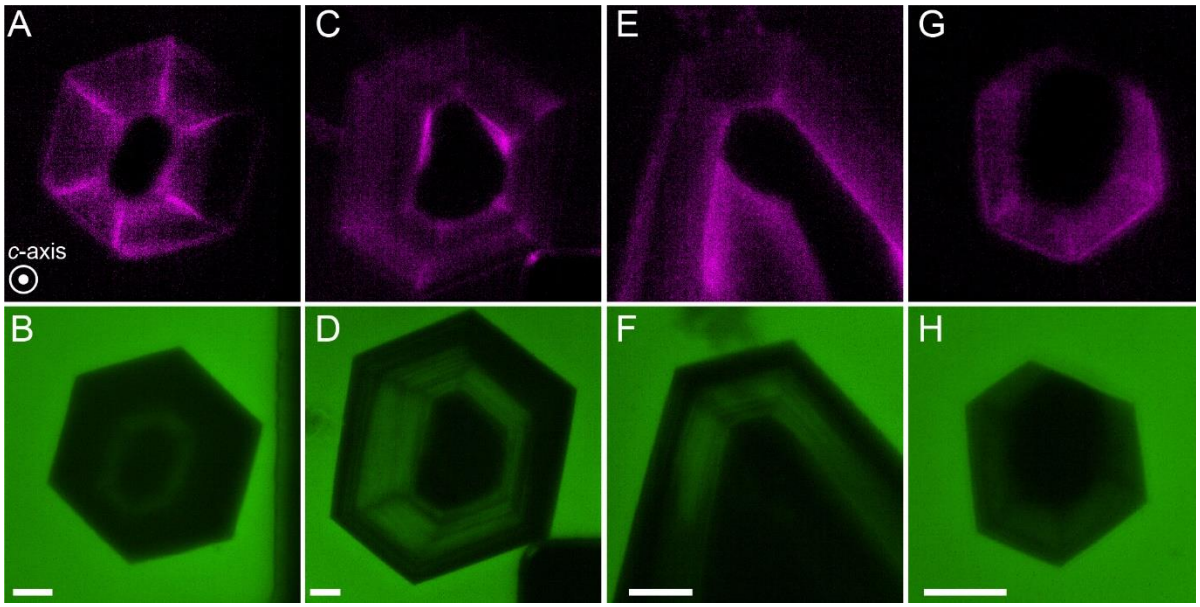

Figure 16: Images of Planar Binding of a Mixture of AFPIII-SP and AFPIII-QAE. Each vertical panel (A,B; C,D; E,F; G,H) depict the same crystal under different light. Crystals A, C, E, and G, depicted in the upper horizontal panel in pink, represent AFPIII-QAE binding, while B, D, F, and H, depicted in the lower, horizontal column in green, represent AFPIII-SP.

The images in Figure 16 represent a mixture of AFPIII-SP and AFPIII-QAE stained with different dyes. The initial concentration used for AFPIII-SP in the mixture was 0.125 mg/mL, while that of AFPIII-QAE was 0.028 mg/mL. However, the concentration of protein reflected in the image might be lower by 20 percent of the initial value. The images in the top panel exhibit the binding of AFPIII-QAE on ice, which was labeled with TRITC (shown in pink). The images in the bottom panel show AFPIII-SP, which was labeled with FITC (shown in green). Each vertical panel represents the same ice crystal, with images taken at the respective fluorescent signal. The scale bar is 10 nm, and the crystal's *c*-axis is pointing out of the page.

The major discrepancy between the images in the upper and lower panels is that the intensity of the fluorescence of AFPIII-QAE is significantly greater than the fluorescent dye on AFPIII-SP in specific locations. For instance, in the images of AFPIII-QAE, there is a

strong signal on the prism plane, evident in the image as the six edges of the hexagon. However, there is no signal on the prism plane of the AFPIII-SP. This is most clear in comparing images A and B, where the hexagonal shape of ice in the former exhibits its strongest signal on the corners of the hexagon, while in the latter, there is no signal at all. These images further confirm previous assertions of alternate plane binding between active and passive isoforms (Takamichi 2009), as well as suggest that perhaps this phenomenon plays a role in the synergistic mechanism of antifreeze proteins.

(v) Discussions

The presence of synergistic, antagonistic, and additive activity among varying protein mixtures provides insight into how binary mixtures inhibit ice growth. Because the structures of the proteins in the binary mixtures tested differ drastically, unlike the previous experiments which observed synergy between $AFGP_{1-5}$ and $AFGP_{7-8}$ and between AFPIII-QAE and AFPIII-SP (Osuga 1978, Takamichi 2009), we can infer that the proteins are not interacting with each other, but rather with the surface of the ice. To elucidate the mechanism by which they interact, which may result in either synergy, antagonism, or an additive effect, we propose two concurrent properties that are at play in protein binding: the speed of protein binding, and the planes to which they bind.

When the proteins in a mixture bind to different planes, as is the case with binary mixtures of AFPIII-SP with *Lp*AFP, $AFGP_{1-5}$, and AFPIII-QAE, as well as mixtures of $AFGP_{7-8}$ with AFPIII-QAE or $AFGP_{1-5}$, the foremost factor for consideration is the adsorption rate of the protein to ice. The active forms have high adsorption rates, and thus bind to the prism plane rapidly, thereby slowing ice growth sufficiently to allow the binding of the passive isoform to

the pyramidal ice-crystal plane. This allows the formerly passive isoform to exhibit significant ice inhibiting properties, and thus high levels of TH activity.

The anomaly to this pattern is AFPI, which when mixed with AFPIII-SP showed an additive effect, but when mixed with $AFGP_{7\text{-}8}$, was antagonistic. Because AFPI does not bind to the prism plane, it is likely that in order for an active protein, regardless of its level of TH activity, to induce synergy in a mixture, it must be capable of binding to the prism plane. Because AFPI does not, it is incapable of inducing synergy in binary mixtures. Therefore, the phenomenon of synergy can be described as uncompetitive binding, as the binding of one protein to an ice-crystal plane increases the number of binding sites of the other protein. This can be depicted as follows:

$$\begin{matrix} Protein\ 1 + ice \\ Protein\ 2 + Ice \end{matrix} \xrightarrow{k_1, k_2} Protein\ 1 - Ice - Protein\ 2$$

The complex formed, which shows synergy, is the product of Protein 1, which has a high adsorption rate and can bind to the prism plane of a crystal, and protein 2, a passive isoform which binds to the pyramidal plane only.

Antagonism is therefore a byproduct of proteins competing for the same binding planes, and thus can be referred to as competitive binding. Because the prism plane has limited binding sites, when two proteins bind to the prism plane, the resultant activity will be lower than expected. This was observed when $AFGP_{1\text{-}5}$ and AFPIII-QAE, two active isoforms with high adsorption rates and high affinity to the prism plane, were mixed, as well as with binary mixtures of $AFGP_{7\text{-}8}$ with *Lp*AFP and AFPI. $AFGP_{7\text{-}8}$ binds to the prism plane, and thus exhibited antagonism when mixed with *Lp*AFP. AFPI and $AFGP_{7\text{-}8}$ both bind to the pyramidal plane, and thus antagonism was observed in that mixture as well. ($AFGP_{7\text{-}8}$ was able to produce

synergy when mixed with $AFGP_{1\text{-}5}$ and AFPIII-QAE despite its ability to bind to the prism plane due to its comparatively low adsorption rate to the two active isoforms). This competitive binding can be explained as follows:

$$Protein\ 1 + ice \overset{k_1}{\rightarrow} Protein\ 1 - ice$$

$$Protein\ 2 + ice \overset{k_2}{\rightarrow} Protein\ 2 - ice$$

Each protein genre binds to the same ice-crystal plane independently of one another, and thus competes to occupy the same space, and is antagonistic to the other.

Microfluidics experiments elucidated the synergistic mechanism even further. The binding of AFPIII-SP is limited to the pyramidal crystal-plane. Therefore, in the absence of an active form, it has limited binding sites, as there are few pyramidal turfs available (Figure 17a). However, in the presence of an active protein which can bind to the prism plane, many more turfs can exist, and therefore, passive AFPIII-SP has many more pyramidal surfaces to which it can bind (Figure 17b).

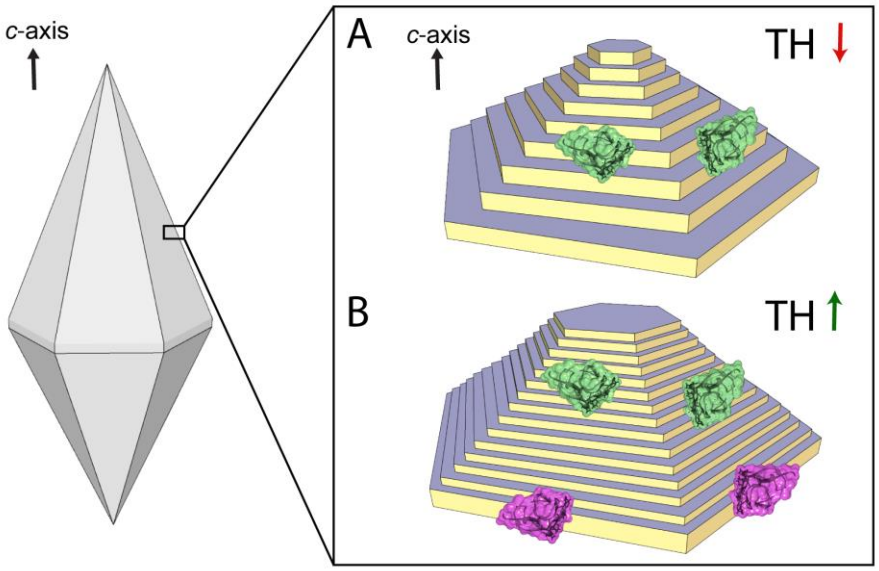

Figure 17: Schematic representation of the binding of a binary mixture of AFGPIII QAE and AFPIII-SP. (A) depicts the binding of green AFPIII-SP alone. (B) illustrates the binding of APIII-SP in the presence of pink AFPIII-QAE. Note the difference in turf number between figure A and B.

(vi) Conclusion

For the first time, synergy has been shown between different types of AF(G)Ps, and our suggested model explains the mechanism by which two isoforms of AF(G)Ps can act synergistically to help fish survive subfreezing temperatures. It is likely that fish evolved with the abundance of the passive isoform as that provides an easier mechanism to control protein activity. These mechanisms can be useful in applications of AF(G)Ps, as mixtures of different AF(G)Ps can be mixed to induce the highest activity at the lowest protein concentrations.

(vii) References

1. Arny, D. C., & Lindow, S. E. (1977). U.S. Patent No. 4,045,910. Washington, DC: U.S. Patent and Trademark Office.
2. Ba, Y., Wongskhaluang, J., & Li, J. (2003). Reversible Binding of the HPLC6 Isoform of Type I Antifreeze Proteins to Ice Surfaces and the Antifreeze Mechanism Studied by Multiple Quantum Filtering−Spin Exchange NMR Experiment. *Journal of the American Chemical Society*, *125*(2), 330-331.
3. Bar Dolev, M., Braslavsky, I., & Davies, P. L. (2016). Ice-binding proteins and their function. *Annual Review of Biochemistry*, 85, 515-542.
4. Bar-Dolev, M., Celik, Y., Wettlaufer, J. S., Davies, P. L., & Braslavsky, I. (2012). New insights into ice growth and melting modifications by antifreeze proteins. *Journal of the Royal Society Interface*, 9(77), 3249-3259.
5. Boonsupthip, W., & Lee, T. C. (2003). Application of antifreeze protein for food preservation: Effect of type III antifreeze protein for preservation of gel-forming of frozen and chilled actomyosin. *Journal of food science*, *68*(5), 1804-1809.
6. Braslavsky, I., & Drori, R. (2013). LabVIEW-operated novel nanoliter osmometer for ice binding protein investigations. *JoVE (Journal of Visualized Experiments)*, (72), e4189.
7. Celik, Y., Drori, R., Pertaya-Braun, N., Altan, A., Barton, T., Bar-Dolev, M., ... & Braslavsky, I. (2013). Microfluidic experiments reveal that antifreeze proteins bound to ice crystals suffice to prevent their growth. *Proceedings of the National Academy of Sciences*, *110*(4), 1309-1314.
8. Davies, P. L. (2014). Ice-binding proteins: a remarkable diversity of structures for stopping and starting ice growth. *Trends in Biochemical Sciences*, 39(11), 548-555.
9. Devries, A. L. (1971). Glycoproteins as biological antifreeze agents in Antarctic fishes. *Science*, *172*(3988), 1152-1155.
10. Raymond, J. A., & DeVries, A. L. (1977). Adsorption inhibition as a mechanism of freezing resistance in polar fishes. *Proceedings of the National Academy of Sciences*, *74*(6), 2589-2593.
11. DeVries, A. L., & Wohlschlag, D. E. (1969). Freezing resistance in some Antarctic fishes. *Science*, 163(3871), 1073-1075.
12. Drori, R., Davies, P. L., & Braslavsky, I. (2015). When are antifreeze proteins in solution essential for ice growth inhibition?. *Langmuir*, 31(21), 5805-5811.
13. Drori, R., Li, C., Hu, C., Raiteri, P., Rohl, A. L., Ward, M. D., & Kahr, B. (2016). A supramolecular ice growth inhibitor. *Journal of the American Chemical Society*, *138*(40), 13396-13401.
14. Esser-Kahn, A. P., Trang, V., & Francis, M. B. (2010). Incorporation of antifreeze proteins into polymer coatings using site-selective bioconjugation. *Journal of the American Chemical Society*, *132*(38), 13264-13269.

15. Farmanesh, S., Ramamoorthy, S., Chung, J., Asplin, J. R., Karande, P., & Rimer, J. D. (2013). Specificity of growth inhibitors and their cooperative effects in calcium oxalate monohydrate crystallization. *Journal of the American Chemical Society*, *136*(1), 367-376.
16. Gilbert, J. A., Hill, P. J., Dodd, C. E., & Laybourn-Parry, J. (2004). Demonstration of antifreeze protein activity in Antarctic lake bacteria. *Microbiology*, *150*(1), 171-180.
17. Knight, C. A. (2000). Structural biology: adding to the antifreeze agenda. *Nature*, 406(6793), 249.
18. Knight, C. A., Cheng, C. C., & DeVries, A. L. (1991). Adsorption of alpha-helical antifreeze peptides on specific ice crystal surface planes. *Biophysical Journal*, 59(2), 409-418.
19. Knight, C. A., Driggers, E., & DeVries, A. L. (1993). Adsorption to ice of fish antifreeze glycopeptides 7 and 8. *Biophysical Journal*, 64(1), 252-259.
20. Nutt, D. R., & Smith, J. C. (2008). Dual function of the hydration layer around an antifreeze protein revealed by atomistic molecular dynamics simulations. *Journal of the American Chemical Society*, *130*(39), 13066-13073.
21. Mochizuki, K., & Molinero, V. (2018). Antifreeze glycoproteins bind reversibly to ice via hydrophobic groups. *Journal of the American Chemical Society*, 140(14), 4803-4811.
22. Osuga, D. T., Ward, F. C., Yeh, Y., & Feeney, R. E. (1978). Cooperative functioning between antifreeze glycoproteins. *Journal of Biological Chemistry*, *253*(19), 6669-6672.
23. Patterson, J. L., & Duman, J. G. (1979). Composition of a protein antifreeze from larvae of the beetle, Tenebrio molitor. *Journal of Experimental Zoology*, *210*(2), 361-367.
24. Reidhead, P. (2006, December 7). Unilever (Breyers and Good Humor) Using Genetically Modified Fish "Antifreeze" Proteins in Ice Creams. Retrieved from http://www.saynotogmos.org/ud2006/antifreeze.pdf.
25. Robinson, C. H. (2001). Cold adaptation in Arctic and Antarctic fungi. *New Phytologist*, *151*(2), 341-353.
26. Takamichi, M., Nishimiya, Y., Miura, A., & Tsuda, S. (2009). Fully active QAE isoform confers thermal hysteresis activity on a defective SP isoform of type III antifreeze protein. *The FEBS journal*, *276*(5), 1471-1479.
27. Wang, T., Zhu, Q., Yang, X., Layne Jr, J. R., & DeVries, A. L. (1994). Antifreeze glycoproteins from antarctic notothenioid fishes fail to protect the rat cardiac explant during hypothermic and freezing preservation. *Cryobiology*, *31*(2), 185-192.
28. Whitesides, G. M. (2006). The origins and the future of microfluidics. *Nature*, *442*(7101), 368.
29. Wowk, B., Leitl, E., Rasch, C. M., Mesbah-Karimi, N., Harris, S. B., & Fahy, G. M. (2000). Vitrification enhancement by synthetic ice blocking agents. *Cryobiology*, *40*(3), 228-236.

30. Yeh, Y., & Feeney, R. E. (1996). Antifreeze proteins: structures and mechanisms of function. *Chemical Reviews*, 96(2), 601-618.
31. Zepeda, S., Yokoyama, E., Uda, Y., Katagiri, C., & Furukawa, Y. (2008). In situ observation of antifreeze glycoprotein kinetics at the ice interface reveals a two-step reversible adsorption mechanism. *Crystal Growth and Design*, 8(10), 3666-3672.